

## Investigation of MHD activity caused by Shattered Pellet Injection via JOREK 3D non-linear MHD simulations

D. Hu<sup>1</sup>, E.Nardon<sup>2</sup>, G.T.A. Huijsmans<sup>2</sup>, M. Lehnens<sup>1</sup>, D. C. van Vugt<sup>3</sup>.

<sup>1</sup> ITER Organization, Route de Vinon sur Verdon, CS 90 046,

13067 Saint Paul-lez-Durance, Cedex, France

<sup>2</sup> CEA, IRFM, F-13108 Saint-Paul-Lez-Durance, France

<sup>3</sup> Eindhoven University of Technology, De Rondom 70 5612 AP Eindhoven

### Introduction

Shattered Pellet Injection (SPI) is the baseline concept for ITER disruption mitigation. The ITER system aims on injecting about  $10^{25}$  atoms on a millisecond timescale. Comparing with the established Massive Gas Injection (MGI) technique, SPI is shown to exhibit better penetration, faster assimilation and more efficient mixing [1]. It is desirable for us to acquire a better understanding about the MHD activities stimulated by the injection, as they are important both to the triggering of thermal quench (TQ) and the particle mixing afterward. This will be the focus of the study presented here on simulations of deuterium SPI into a JET plasma.

### System of interest

We use the 3D nonlinear reduced MHD code JOREK to conduct the simulation. We formulate the problem by considering the reduced MHD with a diffusive neutral species, as is described in Ref. [2]. All neutral convective effects are dropped. The pellet ablation is modelled by considering the strong neutral gas shielding (NGS) model in a Maxwellian plasma [3]. The ablated neutrals are then assumed to deposit with a Gaussian shaped distribution function around the pellet. Meanwhile, the pellet radius evolution is guided by the conservation of mass.

We use the JET shot No. 86887 as a template for the so called “standard equilibrium”, with  $q_0 = 0.935$  and  $q_{95} = 2.9$ . The toroidal magnetic field  $B_t \simeq 2T$ , and the total plasma current is  $I_p \simeq 2MA$ . The plasma is in L-mode before injection, with central electron temperature  $T_e(0) \simeq 1.25keV$ , and central plasma density  $n_e(0) \simeq 2.9 \times 10^{19}/m^3$ . No background impurity radiation is assumed. This particular equilibrium is stable to large scale tearing modes, and the spontaneous sawtooth period is long comparing with the timescale we are considering here.

The pellet shards are injected from the LFS along a major radius, with  $0.5 \times 10^{23}$  particles, the injection speed is  $500m/s \pm 100m/s$  and with a velocity vertex angle of 40 degrees. The injected quantity is shattered into 100 equal sized pieces with  $1.26mm$  radius each.

### Different MHD behavior between MGI and SPI

Different MHD behaviors have been identified by comparing the same quantity SPI and MGI into the standard equilibrium, as is shown in Fig. 1. For the MGI, the 2/1 mode is dominant, and the triggering of the disruption is determined by its growth [2]. The disruption occurs when the mode grows to a critical amplitude to drive up the rest of the spectrum (the timescale is about  $5ms$ ). On the other hand, the MHD stirred up by SPI has a broad spectrum of modes without any dominant one, and the thermal quench starts as the shards enter the  $q = 1$  surface (which takes about  $0.7ms$ ), destabilizing the 1/1 mode, and collapsing the central temperature. The MHD is milder since the pellet travel time is smaller than the tearing mode growth time (milliseconds).

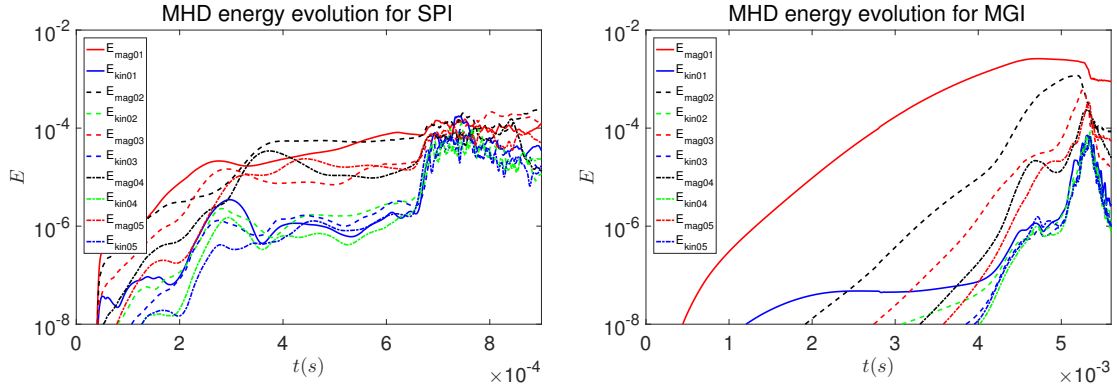


Figure 1: The perturbed magnetic and kinetic energy evolution following (a) the SPI and (b) the MGI.

The reason for this difference in MHD behavior lies in the form of the current perturbation. Due to the mild radiation of deuterium, the mean electron temperature remains of  $\mathcal{O}(100\text{eV})$  even in the wake of shards. Thus the timescale of current contraction is longer than the pellet travel time (it takes about 2.5ms for the current channel to contract into the  $q = 2$  surface), and the contraction is insignificant by the time the shards enter the  $q = 1$  surface, as shown by the  $n = 0$  current profile in Fig. 2, where the red solid line represents the profile just before the TQ.

Meanwhile, the local helical cooling by shards at each rational surface is significant, and creates a helical current perturbations on a much faster timescale due to the small spatial scale. As the ablated pellet atoms ionize, the electron temperature will be flattened along field lines by parallel heat conduction. On irrational surfaces, this only result in the cooling down of the whole surface. Near rational surfaces however, a helical temperature perturbation occurs instead, which relaxes now on a perpendicular transport timescale, as can be seen from the perturbed  $T_e$  profile in Fig. 3. This helical cooling will create a negative helical current perturbation, which is strongly destabilizing to resonant tearing modes [4]. Hence as the shards travel inward, they will destabilize a broad spectrum of neighboring resonant tearing modes, destroying the surfaces by overlapping. This mechanism weakens as the perpendicular conduction rises.

Thus we conclude that the dominant destabilizing mechanism of deuterium SPI is the local helical cooling at rational surfaces, as opposed to the global current contraction, so long as the contraction time is slow comparing with the pellet travel time.

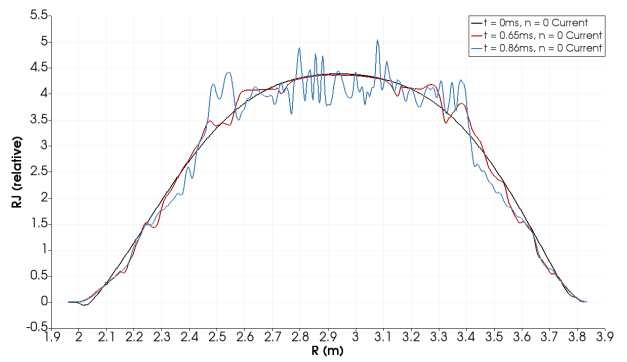


Figure 2: The evolution of  $n = 0$  toroidal current before (red) and after (blue) the thermal quench.

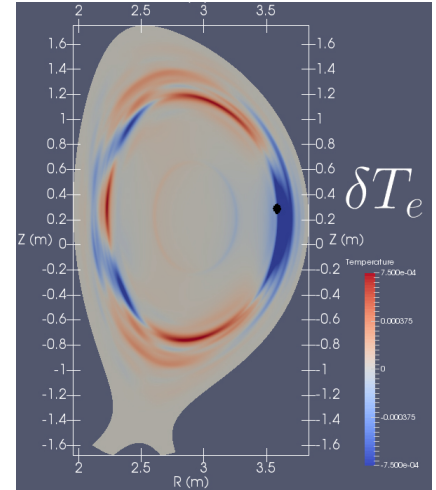


Figure 3: The perturbed temperature showing helical structures at each rational surface. The black dot shows the neutral density peak.

## The injection penetration of SPI and MGI

Apart from the MHD behaviors themselves, we are also concerned with the penetration of the injection. Here, we compare the injection penetration into the plasma core by looking into the density increase at the axis and within the  $q = 1, 3/2, 2$  surfaces as a result of MGI and SPI. As a comparison, we also include the SPI case without any MHD instabilities to see the additional mixing caused by them. The minor radius location of those three surfaces are approximately  $r \simeq 0.26m$ ,  $r \simeq 0.6m$  and  $r \simeq 0.71m$  respectively.

The density profile on the midplane before and after the thermal quench is shown in Fig. 4 for both the SPI and the MGI cases, with vertical dashed and chained lines denote the position of the  $q = 1$  and  $q = 2$  surface respectively. The pre-TQ and post-TQ time is  $0.67ms$  and  $1.05ms$  for the SPI,  $5.37ms$  and  $6.07ms$  for the MGI. It is evident that SPI delivers the injected material far deeper than MGI does, even before the thermal quench, and more so after the thermal quench. It can be seen that a significant mixing and increase of density happens in the plasma core at the end of the quench, and the core density is even higher than the average since pellets penetrate deep into the core and keep ablating there.

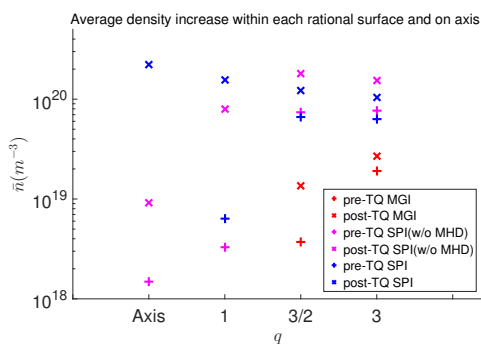


Figure 5: The injection penetration.

The core density change remains minimal despite MHD mixing during the thermal quench. Meanwhile, the SPI shows much better penetration compared with the MGI as pellets deposit right near the core of the plasma, and the MHD during thermal quench contributes to a further increase of penetration as shown by comparing the SPI cases with and without MHD.

## The injection penetration for different temperatures before the thermal quench

The impact of different target equilibrium temperature to the assimilation rate and penetration of the pellets are also of interest. To study this, we simulated SPI into three different equilibria with exactly the same density and temperature profile shape, but different absolute values. The first is our standard equilibrium; the second is the “high  $n_e$ ” equilibrium while keeping the pressure unchanged, so that  $T_e(0) = 420eV$  and  $n_e(0) = 8.7 \times 10^{19}/m^3$ ; the third is the “high  $T_e$ ” equilibrium, with  $T_e(0) = 3.75keV$  and  $n_e(0) = 2.9 \times 10^{19}/m^3$ . It should be noted that these parameters here are still quite below that of a high performance JET DT plasma. The penetration into  $q = 1, q = 3/2$  and  $q = 2$  surfaces just before the TQ is shown in Fig. 6.

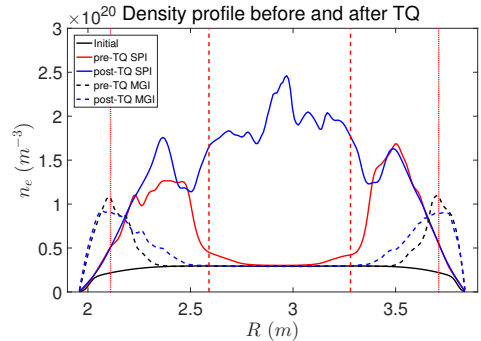


Figure 4:  $n_e$  profile before and after the TQ.

To better represent the injection penetration, the increase of average density at the axis and within the  $q = 1, q = 3/2$  and  $q = 2$  surfaces is investigated both before and after the thermal quench for the MGI case, SPI case and a comparison case where the MHD activities are turned off for SPI, as is shown in Fig. 5. It can be seen that for MGI, most of the injected particles accumulate at the outer part of the plasma, the penetration within the  $q = 1$  surfaces is so small that it cannot be seen on the figure.

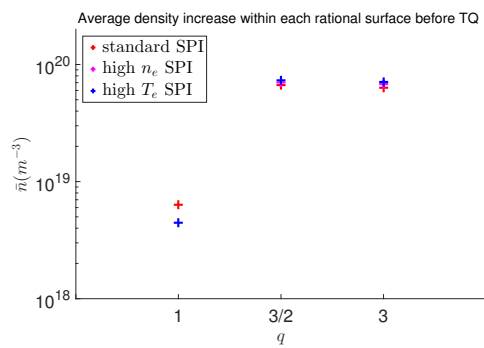


Figure 6: Density rise for different equilibria.

Surprisingly, the three equilibria do not show a significant difference in density increase before the thermal quench. Despite the NGS model for single pellet having a strong power dependence on the plasma temperature [3], such strong dependence is nowhere to be found in the simulation. A potential explanation of this finding is that the parallel heat goes as  $T_e^{5/2}$  in the collisional regime [5]. Thus the

Figure 6: *Density rise for different equilibria.* periphery shards will act as a thermal shield for the inner shards since they create a local low  $T_e$  region so long as the mean free pass of the incoming electrons is not enough to pass the line integrated density created by all the neighboring shards. This should not be confused with the neutral gas & plasma shielding model where the plasmoid sheath is not in thermal equilibrium with the background plasma. This mechanism may fail if the  $T_e$  is high enough (e.g. 10keV) as the high mean free path electrons will bypass the shielding. Further studies will be required to conclude on this result.

## Conclusion

Deuterium SPI into a JET plasma has been simulated using JOREK to study the MHD behavior and the impact on material penetration.. The dominant destabilizing mechanism is found to be the local helical cooling at each rational surface, as opposed to the global current contraction, which has a longer timescale. The resulting different MHD behaviors predicted by this model might be identified experimentally by looking at the magnetic diagnostics or the different asymmetric behaviors caused by MHD modes.

The SPI results in much better penetration compared with the MGI even before the onset of the thermal quench, due to the direct deposition near the plasma core. A significant core density rise is seen for the SPI case during the thermal quench, both due to continued core deposition and MHD mixing. This is beneficial for the runaway suppression as the relativistic electron collision rate (thus the critical electric field for runaway avalanche) is proportional to  $n_e$ .

The SPI penetration before the thermal quench for different equilibrium temperatures has also been studied. No significant difference is found in terms of density rise before the thermal quench. This is potentially caused by the thermal shielding of the pellets cloud which reduce the heat conduction to the inner pellets, thus reducing their ablation rate.

*ITER is a Nuclear Facility INB-174. The views and opinions expressed herein do not necessarily reflect those of the ITER Organization or the European Commission.*

## References

- [1] N. Commaux, D. Shiraki, L.R. Baylor, et al., "First demonstration of rapid shutdown using neon shattered pellet injection for thermal quench mitigation on DIII-D". *Nucl. Fusion* **56** 046007 2016;
- [2] E. Nardon, A. Fil, M. Hoelzl, et al., "Progress in understanding disruptions triggered by massive gas injection via 3D non-linear MHD modelling with JOREK". *Plasma Phys. Control. Fusion* **59** 014006 2017;
- [3] K. Gál, É. Belonohy, G. Kocsis, et al., "Role of shielding in modelling cryogenic deuterium pellet ablation". *Nucl. Fusion* **48** 085005 (2008);
- [4] D. Hu and L. E. Zakharov, "Quasilinear perturbed equilibria of resistive unstable current carrying plasma", *J. Plasma Phys.* **81** 515810602 (2015);
- [5] S. I. Braginskii, "Transport Processes in a Plasma", *Rev. Plasma Phys.* **1**, 205, 1965;